

Piezoelectric mechanism for the orientational pinning of bilayer Wigner crystals and stripes in a GaAs matrix

D. V. Fil

Institute for Single Crystals National Academy of Sciences, Lenin av. 60, 61001, Kharkov, Ukraine

Abstract

We investigate the phonon mechanism for the orientational pinning of Wigner crystals and stripes in two-dimensional electron layers in GaAs matrices. We find the orientation of bilayer Wigner crystals on the (001), (111), (0 $\bar{1}$ 1) and (311) interfaces versus the interlayer distance and determine the regions of parameters, where polydomain structures can emerge. For the stripe states in electron layers situated close to the (001) surface we show that the interference between the piezoelectric and deformation potential interaction may be responsible for the preferable orientation of the stripes along the [110] direction. For the bilayer system on the (001) interfaces we predict the suppression of the resistance anisotropy.

Key words: Wigner crystal, stripe structure, piezoelectricity

PACS: 73.21.Fr, 73.40.Kp

1 Introduction

Due to the number of technological advantages AlGaAs heterostructures are the most widely used systems to construct two-dimensional electron layers. Low level of disorder in this systems make it possible to realize the states with nonuniform spatial distribution of electrons. The formation of these states is regulated by the Coulomb interaction, which, under certain conditions, forces the transition into the Wigner crystal or the stripe state. Since in cubic crystals the Coulomb interaction is the isotropic one, the energy of such states does not depend, in the first approximation, on their orientation relative to the crystallography axes of the host matrix. Nevertheless, experimental studies of the resistance anisotropy in high Landau levels [1–3] (which is considered as an indication of the stripe state) show that certain orientational symmetry-breaking mechanisms exist.

In this paper we consider the electron-phonon interaction as a possible origin of the native anisotropy. The main source of the anisotropy is the piezoelectric interaction, which remains anisotropic in cubic systems. This mechanism was studied by Rashba and Sherman [4,5]. In [4,5] the influence of the piezoelectricity on the structure and orientation of monolayer Wigner crystals in isotropic piezoelectrics was investigated. Since in GaAs crystals the anisotropy of the elastic moduli is quite large, the results of [4,5] cannot be applied directly to them. In this paper, using the approach slightly different from [4,5], we consider the model, where the anisotropy of the elastic moduli of GaAs is taken into account. In section 2 the model is applied to the study of orientation of bilayer Wigner crystals. Technical details of the calculations were given in Ref. [6]. Here we mainly concentrate on the results. For the bilayer systems on the (001), (111), ($\bar{0}\bar{1}1$) and (311) interfaces we find the stable and metastable orientations of the Wigner crystal versus the interlayer separation and determine the regions of parameters, where polydomain Wigner crystal structures can be realized.

In section 3 we address the problem of stripe orientation in high Landau levels. It was shown in [7] that in an electron layer parallel to the (001) crystallography plane the piezoelectricity causes the preferential orientation of the stripes along the [110] or the $[\bar{1}10]$ direction, while the piezoelectric mechanism alone does not explain further lowering of the symmetry of the interaction (in magnetic field perpendicular to the layer the [110] orientation is only observed). We extend the model of Ref. [7] and take into account the piezoelectric as well as the deformation potential interaction. It is shown that for the electron layers situated near the surface of the sample these two channels of the electron-phonon interaction are strongly interfere and due to this effect the C_{4v} symmetry of the electron-electron interaction is reduced to the C_{2v} one. We also analyze the orientation of the stripes in the electron layers parallel to the (111), ($\bar{0}\bar{1}1$) and (311) crystallography planes, and in bilayer systems.

2 Piezoelectric mechanism of orientation of bilayer Wigner crystals

The electrostatic potential φ of an electron in a piezoelectric matrix can be found from the solution of the following equations:

$$\nabla \mathbf{D} = 4\pi e \delta(\mathbf{r}), \quad (1)$$

$$\frac{\partial \sigma_{ik}}{\partial x_k} = 0, \quad (2)$$

where $D_i = -\varepsilon \partial_i \varphi - 4\pi \beta_{i,kl} u_{kl}$ is the electric displacement vector, $\sigma_{ik} = \lambda_{iklm} u_{lm} - \beta_{l,ik} \partial_l \varphi$, the stress tensor, ε , the dielectric constant, λ_{iklm} , the elastic

moduli tensor, $\beta_{i,kl}$, the piezoelectric moduli tensor, u_{ik} , the strain tensor.

Solving Eqs. (1,2) one can present the electron-electron interaction potential in the form:

$$V(\mathbf{r}) = \frac{e^2}{\varepsilon r} - \chi \frac{e^2}{\varepsilon r} \sum_{n \geq 0} \sum_{|m| \leq n} A_{nm} Y_{nm}(\Theta_{\mathbf{r}}, \phi_{\mathbf{r}}) + O(\chi^2) \quad (3)$$

where $Y_{nm}(\theta, \phi)$ are the spherical harmonics, $\chi = e_{14}^2 / \varepsilon c_{11}$ (here and below the cubic symmetry of the host matrix is assumed). For the case of an anisotropic crystal ($c_{11} \neq c_{12} + 2c_{44}$) the coefficients A_{nm} are computed numerically.

The second term in r.h.s. of Eq. (3) describes the second order correction to the electron-electron interaction caused by the virtual exchange of acoustic phonons. This term contains the dependence on the direction of the bond.

The lattice sum for the interaction (3) can be reduced to the rapidly convergent form (see Ref. [6]). Using the rapidly convergent form we have computed the energy of the bilayer Wigner crystal and found its stable and metastable orientations versus the parameter $\eta = d\sqrt{n/2}$ (d is the interlayer distance, and n is the electron density). In principle, the piezoelectric interaction may influence on the symmetry of the electron lattice as well, but for GaAs, where the parameter χ is small ($\approx 2 \cdot 10^{-4}$), this effect is negligible, and the phase diagram is almost the same as in case of pure Coulomb interaction [8].

For the calculations we use the elastic moduli of GaAs: $c_{11} = 12.3 \cdot 10^{10} \text{ N/m}^2$, $c_{12} = 5.7 \cdot 10^{10} \text{ N/m}^2$, $c_{44} = 6.0 \cdot 10^{10} \text{ N/m}^2$. We would like to note that the results do not change qualitatively under the 10% variation of c_{ik} . Therefore, one can neglect a small difference of c_{ik} in pure GaAs and in AlGaAs. The results of the calculations for the (001), (111), (0 $\bar{1}$ 1), and (311) interfaces are presented in Fig. 1, where the most preferable orientation of the shortest primitive lattice vector is shown. One can see that in general case the orientation of the bilayer Wigner crystal is sensitive to the interlayer separation. A common feature of the dependences presented is a jump-like reorientation under the 1-st order type transition from the rhombic to the hexagonal phase. For the (111) and (0 $\bar{1}$ 1) interfaces a step-like reorientation is also observed under the 2-nd order type transition from the rectangle to the cubic phase.

It is instructive to determine the regions, where a polydomain structure of the bilayer Wigner crystal may emerge. As it follows from Fig. 1 the polydomain structure is expected for the rectangle, rhombic and hexagonal phases in the (001) oriented bilayers, for the rectangle, square and rhombic phases in the (111) bilayers, for the rectangle phase in the (0 $\bar{1}$ 1) bilayers, and for all phases (except the one-component hexagonal) in the (311) bilayer. In the last case the rectangle phase may show such a behavior at $\eta > 0.17$, and the cubic

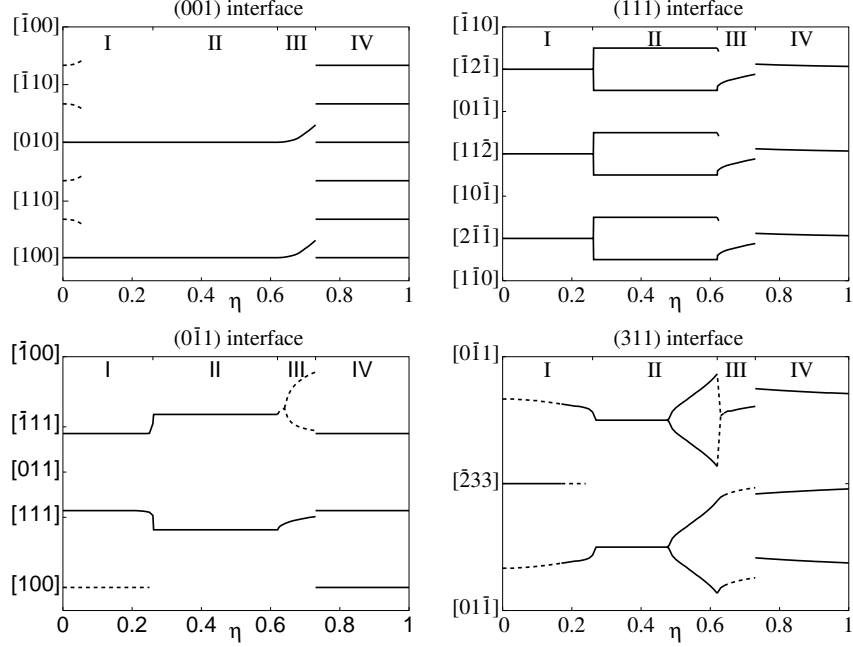


Fig. 1. Direction of the shortest in-layer electron-electron bond versus the inter-layer separation for the bilayer Wigner crystal on the (001), (111), (011), and (311) interfaces. Solid curves correspond to the stable orientation; dotted curves, the metastable one. The Roman numbers indicate the regions, where different types of the electron lattice are realized: I, staggered rectangle; II, staggered cubic; III - staggered rhombic; IV, staggered hexagonal (the one-component hexagonal phase region is too narrow to be shown in this scale)

phase - at $\eta > 0.47$.

3 Piezoelectric mechanism of stripe orientation

In this section we consider the role of the electron-phonon interaction in the orientation of stripe states in high Landau levels. We consider an electron layer situated close to the (001) surface of the sample and take into account two channel (piezoelectric and deformation potential) of the electron-phonon interaction. For the (001) surface the matrix elements of the interaction of the electrons with surface acoustic modes are in-phase for these two channels (see [9]), and the phonon mediated interaction contains the interference term. The interference term may lower the symmetry of the electron-electron interaction.

The potential energy is given by the expression

$$U = \int_{z<0} d^3r \left(\frac{\mathbf{E}\mathbf{D}}{8\pi} + \frac{u_{ik}\sigma_{ik}}{2} \right) + \int_{z>0} d^3r \frac{E^2}{8\pi} + U_{def} , \quad (4)$$

where \mathbf{E} is the electric field, and the deformation potential interaction is chosen in the form

$$U_{def} = \int d^3r \Lambda \rho (u_{xx} + u_{yy}) \delta(z + a) . \quad (5)$$

Here Λ is the deformation potential constant, ρ , the electron density, a , the distance between the electron layer and the surface. Since we consider the model of a zero-thickness electron layer, the interaction with u_{zz} deformations is not included in (5).

The quantities \mathbf{D} and σ_{ik} satisfy the equations $\nabla \mathbf{D} = 0$, $\partial_k \sigma_{ik} = 0$. The boundary conditions at the free surface are the continuity of D_z and E_x , E_y , and the vanishing of σ_{iz} . At $z = -a$ the quantities D_z and σ_{iz} are discontinuous:

$$D_z \Big|_{z=-a+0} - D_z \Big|_{z=-a-0} = 4\pi e \rho , \quad (6)$$

$$\sigma_{iz} \Big|_{z=-a+0} - \sigma_{iz} \Big|_{z=-a-0} = -F_i , \quad (7)$$

where $\mathbf{F} = \Lambda(\partial_x \rho, \partial_y \rho, 0)$ is the tangential force applied to the unit area of the interface. This force is induced by the deformation potential interaction. We should note that discontinuity of the stresses is the consequence of the zero-thickness approximation for the electron layer. Using the boundary conditions specified one can reduce the energy (4) to the form

$$U = \frac{1}{2} \int d^2r (e \rho \varphi - u_i F_i) , \quad (8)$$

where the electrostatic potential φ and the displacement field \mathbf{u} are taken at $z = -a$. The energy (8) can be presented as a sum of a pure Coulomb part (which is isotropic) and a phonon part U_{ph} (which includes the isotropic as well as the anisotropic terms).

For simplicity, we consider the unimodal approximation for the electron density modulation $\rho = \rho_0 \cos \mathbf{q} \mathbf{r}_{pl}$, where the absolute value of \mathbf{q} is determined by the period l of the stripe structure ($q = 2\pi/l$) and its direction is perpendicular to the axis along which the stripes are aligned.

We concentrate on the anisotropic GaAs crystal and compute the values of φ and u_i at $z = -a$ numerically. We use the parameters $e_{14} = 0.15 \text{ C/m}^2$,

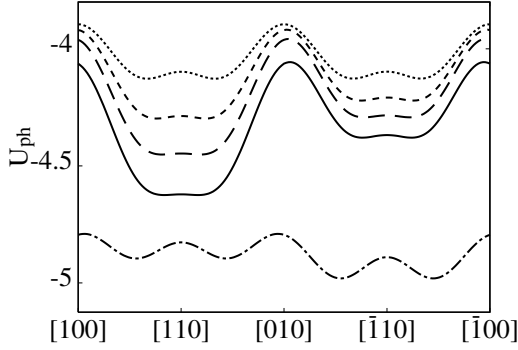


Fig. 2. Phonon contribution to the energy of the stripe phase (in units of χU_c) near the (001) surface versus the direction of the stripes at $a/l = 1.0, 0.6, 0.5, 0.4, 0.2$ (from top to bottom).

$\Lambda = 7.4 \text{ eV}$, $\varepsilon = 12.5$, $l = 2 \cdot 10^3 \text{ \AA}$, and the elastic moduli given above for the calculation. For the (001) surface the dependence of the energy U_{ph} on the direction of stripes is shown in Fig. 2. The values of U_{ph} are given in units of χU_c (per unit area), where $U_c = \pi e^2 \rho_0^2 / 2 \varepsilon q$ is the Coulomb energy at $a/l \gg 1$. Our calculations show that at $a/l > 0.23$ the global minima are reached for two directions symmetrically deviated from the $[110]$ axis on a small angle. In this case one can expect that a domain structure is formed, and, in average, the system should demonstrate the minimum resistance in the $[110]$ direction and the maximum resistance in the perpendicular direction. The calculations predict the largest resistance anisotropy at $a/l = 0.4$. If there is no other sources for the native anisotropy, the high and low resistance directions may alternate at $a/l \approx 0.23$. At $a/l > 1$ the interference term becomes exponentially small and the 4-fold symmetry is restored.

For ρ_0 of order of the average density of electrons at the high half-filled Landau level and $a/l = 0.4$ we estimate the absolute value of the anisotropy (the energy difference of the $[110]$ and $[\bar{1}10]$ oriented stripes) as 0.7 mK per electron, which is comparable with the values given by the other possible mechanism of the anisotropy [10]. The mechanism [10] is connected with the effective mass anisotropy caused by the asymmetry of potential confining the electron in the quantum well. From our estimate we conclude that both mechanisms may work in parallel and in case of the symmetric confining potential [3] the native anisotropy can be accounted for the phonon mechanism. Note that the effect considered depends significantly on the distance between the electron layer and the surface.

Assuming the phonon mechanism plays an important role in the orientational pinning of the stripes, it is interesting to analyze the orientation in electron layers parallel to some other crystallography planes. The results of the cal-

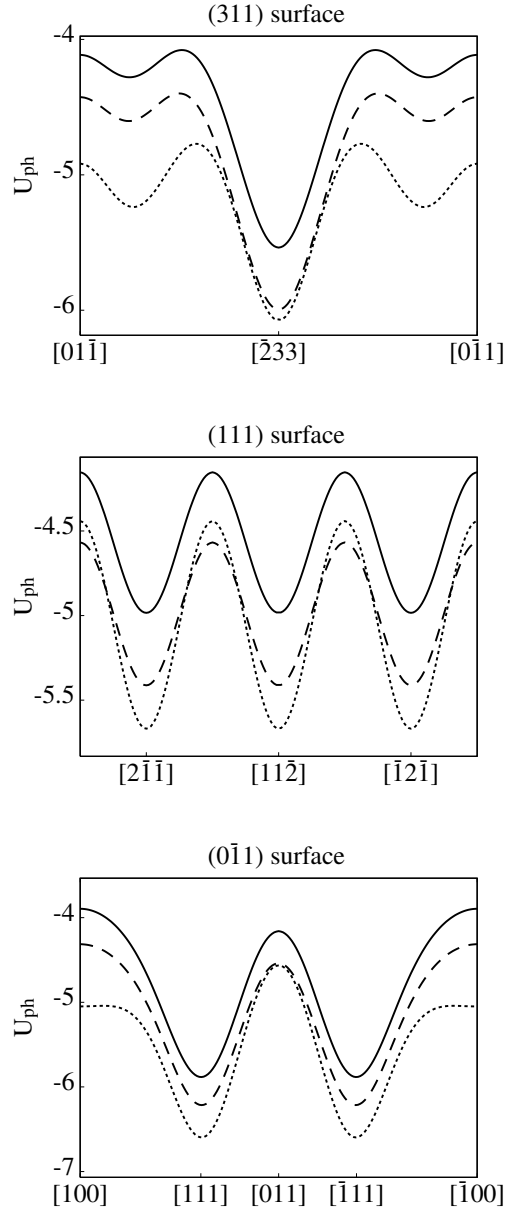


Fig. 3. Stripe energy anisotropy for the (111), $(0\bar{1}1)$ and (311) surfaces. Solid curve - $a/l = 1$, dashed curve - $a/l = 0.4$, dotted curve - $a/l = 0.2$. U_{ph} is in χU_c units.

culations for the (111), $(0\bar{1}1)$ and (311) plane are shown in Fig. 3. In these cases, as it follows from the results presented, the orientation of the stripes does not depend on the ratio a/l . For the (311) surface the phonon mechanism predicts the $[\bar{2}33]$ orientation. This prediction is in agreement with the experiment [11]. The absolute value of the anisotropy for the (311) surface is in several times large then for the (001) one. For the (111) plane the global minima correspond to three different directions of the stripes $([2\bar{1}\bar{1}], [\bar{1}2\bar{1}]$ and

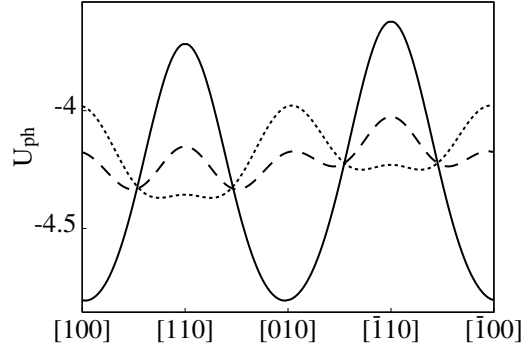


Fig. 4. Stripe energy anisotropy (in χU_c per one layer) for the bilayer system near the (001) surface at $a/l=0.4$. Solid curve - $d/l = 0.5$, dashed curve - $d/l = 1$, dotted curve - $d/l = 2$

$[\bar{1}\bar{1}2]$). In this case the polydomain structures may not show any resistance anisotropy. For the $(0\bar{1}1)$ plane the domains with $[111]$ and $[\bar{1}\bar{1}1]$ orientation are energetically preferable, and the polydomain structure will show the resistance anisotropy with the $[011]$ low resistance direction. The anisotropy is expected to be small due to a large angle ($\approx 70^\circ$) between two preferable orientations.

To complete our study we consider the orientation of stripes in the bilayer systems. Let there are two electron layers on the distances a and $a+d$ from the surface, and the electron density modulation in the one layer is $\rho_1 = \rho_0 \cos \mathbf{q}\mathbf{r}_{pl}$, and in the other layer is $\rho_2 = -\rho_0 \cos \mathbf{q}\mathbf{r}_{pl}$. For the (001) surface the change of the anisotropy under variation of the ratio d/l is shown in Fig. 4. One can see that in the bilayer systems with a polydomain structure the angle between the directions of stripes in different domains becomes larger for smaller d/l . At $d/l = 0.5$ these directions are almost perpendicular to each other. It means that the resistance anisotropy becomes very small. For the (111), $(0\bar{1}1)$ and (311) crystallography planes we do not find any significant changes in the stripe orientation under the variation of the parameter d/l . In these cases the bilayer and monolayer systems will demonstrate the same orientation.

To conclude this section, we would like to point out on the questions, which, in our opinion, require further experimental investigation. 1. Is there a dependence of the resistance anisotropy on the distance between the electron layer and the surface? 2. Do the electron layers on other interfaces demonstrate the resistance anisotropy? 3. Is this effect modified in bilayer systems? Experimental study of these questions may be important for establishing of the mechanism for the orientational symmetry breaking in high Landau levels.

References

- [1] M. P. Lilly, K. B. Cooper, J. P. Eisenstein, L. N. Pfeiffer and K. W. West, Phys. Rev. Lett. **82**(1999) 394.
- [2] R. R. Du, D. C. Tsui, H. L. Stormer, L. N. Pfeiffer, K. W. Baldwin and K. W. West, Solid State Commun. **109** (1999) 389.
- [3] K. B. Cooper, M. P. Lilly, J. P. Eisenstein, T. Jungwirth, L. N. Pfeiffer, K. W. West, Solid State Commun. **119** (2001) 89.
- [4] E. I. Rashba and E. Ya. Sherman, Fiz. Tekh. Poluprovodn. **21** (1987) 1957 [Sov. Phys. Semicond. **21** (1987) 1185].
- [5] E. Ya. Sherman, Phys. Rev. B **52** (1995) 1512.
- [6] D. V. Fil, Fiz. Nizk. Temp. **27** (2001) 523 [Low Temp. Phys. **27** (2001) 384]; *preprint* cond-mat/0104243.
- [7] D. V. Fil, Fiz. Nizk. Temp. **26** (2000) 792 [Low Temp. Phys. **26** (2000) 581]; *preprint* cond-mat/0004107.
- [8] G. Goldoni, F.M.Peeters, Phys. Rev. B **53** (1996) 4591.
- [9] A. Knabchen, Y. B. Levinson, O. Entin-Wohlman, Phys. Rev. B **54** (1996) 10696.
- [10] E. E. Takhtamirov and V. A. Volkov, Pis'ma v Zh. Exp. Teor. Fiz. **71** (2000) 712 [JETP Letters **71** (2000) 422].
- [11] M. Shayegan, H. C. Manoharan, S. J. Papadakis, E. P. De Poortere, Physica E, **6** (2000) 40.